

Structural, optical and morphological properties of zinc -doped cobalt-ferrites $\text{CoFe}_{2-x}\text{Zn}_x\text{O}_4$ ($x=0.1-0.5$)

M. H. Jameel^{a,*}, M. A. Agam^b, M. Q. Hamzah^{b,c}, M. S. Roslan^b,
S. Z. H. Rizvi^b, J. A. Yabagi^d

^a*Nano-optoelectronics Research Laboratory, Department of Physics, University of Agriculture Faisalabad, 38040 Faisalabad, Pakistan*

^b*Department of Physics and Chemistry, Faculty of Applied Sciences and Technology, University Tun Hussein Onn Malaysia, 83000 Malaysia*

^c*General Directorate of Education in Al-Muthanna Governorate, Ministry of Education, Republic of Iraq*

^d*Departments of Physics, Faculty of Natural Sciences, Ibrahim Badamasi Babangida University Lapai, P.M.B 11, Lapai, Niger State, Nigeria*

Cobalt-ferrite (CoFe_2O_4) based nanoparticles are appropriate candidates for electrical, optical, and magnetic applications for electrical appliances. In the current study, a co-precipitation technique was used to prepare Zinc doped cobalt ferrites with compositions $\text{CoFe}_{2-x}\text{Zn}_x\text{O}_4$ ($x=0.1-0.5$) at various percentages using Zinc and Co-nitrate as precursors. The analysis of crystal phase structure, hkl planes, average crystalline size, volume, and lattice parameters of the unit cell of $\text{CoFe}_{2-x}\text{Zn}_x\text{O}_4$ doped (NPs) was carried under X-ray diffraction (XRD). X-ray spectra analysis, FT-IR Spectra, UV Visible Spectra, and SEM studies shown that the as-synthesized powders were contained of nano-crystallite size (42–53nm) cubic-spinel phase with irregularly-structure. Calcination at low temperature (80°C) of the precursor followed through sintering (500°C for 3h) con-sequence in a single-phase cubic-spinel shape with an average particle size of 42-53nm, as shown by scanning electron micrographs images. Sharp peaks and intense diffraction features in XRD pattern show that an increase in Zn doping concentration in cobalt spinel ferrite increases the crystalline behavior of the cubical spine phase. In cubical structure ferrites crystal lattices, the absorption band at low frequency is noticed above 400cm^{-1} but in the range of $300-600\text{cm}^{-1}$ of the Fourier Transform Infrared bands were attributed to the tremblant of the ions of metal. The absorbance results of UV Spectra indicate that Zinc doped Cobalt Ferrite specimen had symbolic absorbance in the range of 660-900nm wavelength range of the conspicuous region. The Zn-doped cobalt-ferrite have a high strain derivative that could be a prospective material for electrical devices.

(Received November 13, 2020; Accepted April 4, 2021)

Keywords: Spinal ferrites, Cobalt ferrites, Morphology, Doping

1. Introduction

Spinal ferrite (SF) nanomaterial's, is a new unique and extraordinary that recently attract material great interest for its myriad applications ranging from high data storage media to rechargeable batteries and from gas sensing to medical diagnostic device applications[1, 2]. The magnetic characteristics of Zn doped cobalt ferrite are governed through their, microstructure, composition, and grain size which can determine by the synthesis method [3- 8]. The improved magnetic properties are detected of reduced grain size and further intrinsic cation distribution between the two sublattices. The General formula for ferrites is AB_2O_4 , where the molecule is formed mainly because of magnetic interaction between cations and magnetic moments which are exist at "A" tetrahedral corners and "B" octahedral [9]. In the spinel structure of $\text{CoFe}_{2-x}\text{Zn}_x\text{O}_4$ "Co" is a divalent atom that occur the tetrahedral corners, whereas Fe is a trivalent atom have

* Corresponding author: mhasnainjamil@gmail.com

place the octahedral B-corners. With A corners being occupied by Fe^{3+} ions, and B corners being placed by Co^{2+} and Fe^{3+} ions, the structure is recognized as inverse spinel ferrites structure [10, 11]. The magnetic and structural situations of these two lattice sites can be controlled by the synthesis technique, chemical configuration, and annealing temperature. Physical properties of $\text{CoFe}_{2-x}\text{Zn}_x\text{O}_4$ can be changed through types of cations substitutions and concentration. Cobalt is considered as high potential dopant material for ferrites because of its high conductivity, good mechanical hardness, chemical stability and reasonable saturation magnetization [12, 13]. Spinel ferrites shape is close cubical structure of 32 anions along 24 cations of oxygen. The eight cations are situated in tetrahedral corners and remaining are located at 16 octahedral corners. Physical characteristics of spinel ferrites depend on distribution of metal ions at various lattice sites, sintering temperature and reaction temperature method of preparation. Zinc ferrite has a nominal spinel structure and Zn^{2+} ions have the end to occupy tetrahedral corners [14, 15]. There are numerous techniques for synthesizing small sized magnetic spinel ferrite particles for example co-precipitation sol-gel, microwave-induced combustion, co-precipitation, standard double-sintering technique, microwave sintering process, reverse micelle reaction process, sol-gel auto-combustion technique, , and evaporation process [16- 18]. Our work is focused on the co-precipitation method for preparation of zinc doped cobalt ferrites. This method is selected for its improved high features homogeneity, purity, and it has the best benefit of simplicity, less expensive, a short waste materials, and an friendly environment process. The structural and good morphological characteristics of the synthesized cobalt ferrite NPs are investigated with numerous characterization methods [19] .

2. Materials and method

In the current study, zinc doped cobalt ferrite was prepared through co-precipitation method at low temperature (80°C). Powder of cobalt chloride hexahydrate ($\text{CoCl}_2 \cdot 6\text{H}_2\text{O}$), zinc sulphate (ZnSO_4) and Iron chloride hexahydrate ($\text{FeCl}_3 \cdot 6\text{H}_2\text{O}$) were weighed on a digital electronic balance according to stoichiometric proportions. All chemical substances such as cobalt chloride hexahydrate ($\text{CoCl}_2 \cdot 6\text{H}_2\text{O}$) is prepared separately in 50ml distilled water stirred continuously were later add 2.0M aqueous solution of NaOH (Sodium hydroxide) as a precipitating agent. The collective dissolved solution was stirred on a stirrer and sodium hydroxide (NaOH) solution was dropwise in to solution [2].

3. Result and Discussion

3.1. XRD Analysis

In XRD Analysis, often abbreviated as XRD Analysis, is a safe and accurate crystal sample examination method used to study the structure of crystalline materials. Sharp crystalline peaks of $\text{CoFe}_{2-x}\text{Zn}_x\text{O}_4$ ($x=0.1-0.5$) appear in the Figure 1 of 5 samples for different concentration of Zn dopant. XRD analysis of all 5 specimens showed the development of the cubic spinel (hard glassy mineral) architecture and phase purity.[20- 22].

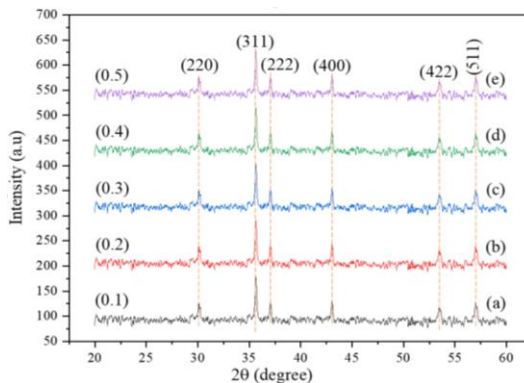


Fig. 1. XRD Pattern of Zinc doped Cobalt Ferrite ($\text{CoFe}_{2-x}\text{Zn}_x\text{O}_4$).

X-Ray Diffraction peaks in Figure 1(a-e) are indicated to (220), (311), (222), (400), (422) and (511) reflection hkl planes of (CoFe_{2-x}) Cobalt ferrite appear at 2θ (Bragg's angle) values of 30.07942° , 35.64743° , 37.06992° , 43.06467° , 53.4488115° and 56.9847° respectively. XRD analysis peaks perfectly matched with the JCPDS Card # 22-1086 suggesting the purity of cubical spinel ferrite structure having 3d symmetry and Fd3m space group. No additional peaks in Fig.1 ascribing the contamination phases in the Zn doped samples signifying the presence of Zn in Cobalt ferrite ($\text{CoFe}_{2-x}\text{Zn}_x\text{O}_4$) matrices. High intensity of the sharp diffraction peak appeared at 35.64743° indexed to (311) plane is allude to be a measure of its perfect crystallinity. Sharper peaks and intense diffraction features in Figure 1(a-e) show that by increasing in the (Zn) zinc concentration the crystalline behavior of the cubical spinel structure of cobalt ferrite increases, indicating evolution of the particles with increased Zn concentration.

The average crystalline size (D) is calculated from XRD analysis for different diffraction angles by using Scherrer's equation. Crystalline size (D) is measured in nano-meter. Lambda (λ) wavelength of X-ray. λ has a typical value of about 1.54\AA . [23] Shape factor (K) has a characteristic value of about (0.9-0.99). The value of shape factor (K) varies with the actual shape of the crystallites [24].

θ is represent of the Bragg's angle. FWHM (β) is represent the line enlargement (bisector) at half the maximum intensity of XRD peak, after deducting the instrumental line increase, in radians (r).

$$D = \frac{K\lambda}{\beta \cos\theta} \quad (1)$$

Lattice constant (a) refers to the physical quantity of unit cells in a crystal lattice. Crystal lattices in 3d generally have 3 lattice constants, referred as a, b and c.

$$a = d\sqrt{h^2 + k^2 + l^2} \quad (2)$$

d-spacing is the interplanar spacing, (h, k, l) are indicated planes and signifies Miller indices adjacent planes. It is concluded that lattice parameter, (a) for $\text{ZnCoFe}_2\text{O}_4$ is in idealistic arrangement having perfect value (8.38\AA) along a tangent [25, 26].

Atomic packing factor of cubical architecture can be calculated through following formula:

$$P = \frac{1 \cdot \frac{4}{3} \pi \left(\frac{1}{2}a\right)^3}{a^3} \quad (3)$$

The volume of unit cell of cubical structure can be calculated through given below equation:

$$V = a^3 \quad (4)$$

Density (ρ_x) of X-ray can be observed by using the following formula:

$$\rho_x = \frac{ZM}{N_A} \quad (5)$$

Z refers to number of atoms present in a unit cell ($Z = 8$), M refers to molecular weight of compound and N_A refers to the Avogadro number.

$$\rho_x = \frac{n M_w}{N_A V} \quad (6)$$

Strain of the unit cell of a crystal lattice can be calculated using the following equation:

$$\text{Strain} = \frac{k\lambda}{D} \quad (7)$$

k is the average FWHM (β).

Table 1. Zn Concentration, Crystallite Size (D), Volume (a^3), Lattice Constant (a), d- Spacing, Strain and Packing Factor calculated for XRD analysis of different specimen.

Zinc Concentration (X)	Crystallite Size D (nm)	Lattice Constant (a=b=c)	Volume a^3 (nm ³)	d Spacing (Å)	Strain	Packing Factor (P)
0.1	37.730	8.369	573.640	2.193	9.78×10^{-04}	0.522
0.2	37.013	8.380	588.450	2.218	1.02×10^{-03}	0.523
0.3	36.073	8.390	590.475	2.223	1.07×10^{-03}	0.524
0.4	35.685	8.399	590.923	2.223	1.09×10^{-03}	0.524
0.5	35.292	8.409	593.329	2.227	1.12×10^{-03}	0.524

In Fig. 2 by increasing the concentration of Zinc ion, lattice parameter (a) of crystal lattice increases so, it conforms Vegard's Law. Increase in "a" lattice constants linearly by increasing zinc ion (Zn^{2+}) concentration specify the amount of crystal lattice increase without any change in the symmetry of crystal lattice.

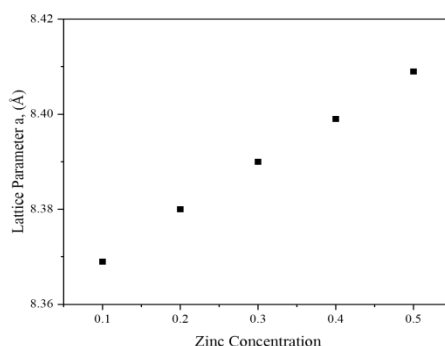


Fig. 2. Lattice parameter, (a) of $CoFe_{2-x}Zn_xO_4$ Zinc doped Cobalt Ferrite, dependency upon the extension of Zinc concentration.

Increase in the crystal lattice constants occur because of the size of zinc ions (Zn^{2+}) ionic radius (0.82Å) that is larger than the ionic radius of cobalt ions (Co^{2+}) (0.78Å). Crystal size for zinc doped cobalt ferrites at different concentration are mentioned in Table 1. Crystal size

observed for ($x = 0.1-0.5$) ferrites samples are 37.73, 37.01, 36.07, 35.69 and 35.29 nm correspondingly. The reduction in the crystal size against rise in the concentration of Zn^{2+} ions is because of lessened bond enthalpy of $Zn^{+2}-O^{-2}$ (159 kJ/mol) corresponding to enthalpy of $Co^{+2}-O^{-2}$ (384 kJ/mol).

3.2. FTIR Spectra

Fourier Transform Infrared Spectroscopy is such a technique used to determine an infrared radiation spectra of emission or absorption of a solid. In Fig 3 Fourier transform infrared spectra of zinc doped cobalt ferrite are noted in the range of $4000-500\text{ cm}^{-1}$. In cubical structure ferrites crystal lattices the absorption band of low frequency is noticed above 400 cm^{-1} . In the region of $300-600\text{ cm}^{-1}$, the bands in FTIR are attributed to the tremblant of the ions of metal.

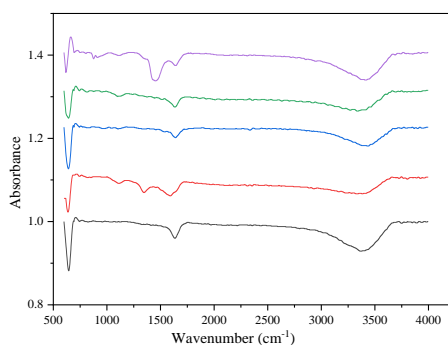


Fig. 3. FTIR Spectra of Zinc doped Cobalt Ferrite ($CoFe_{2-x}Zn_xO_4$) $x=0.1-0.5$ for specimens (a) CoZnF1, (b) CoZnF2, (c) CoZnF3, (d) CoZnF4, and (e) CoZnF5.

Furthermore, FTIR bands noticed at 600 cm^{-1} is ascribed to the stretching tremblant of tetrahedral group of (Cobalt) $Co^{2+}-O^2$. FTIR bands about 1636 cm^{-1} and 3400 cm^{-1} are arise because stretching and bending vibration of water (H_2O) molecules, that indicates the residues of hydroxyl (OH) groups during the preparation of samples [27, 28]. Extremely weak band nearby 1370 cm^{-1} is originate due to the group of nitrates (NO^3) that is anticipated to remain as slight contamination in specimens. Spectra of Fourier Transform Infrared Spectroscopy of Zinc doped Cobalt Ferrite originated insignificant quantity of contamination in the prepared samples of $Co_{1-x}Zn_xFe_2O_4$.

Ultraviolet-Visible Spectrophotometry or Ultraviolet-Visible Spectroscopy allude to reflection or absorption spectroscopy in fragment and entire of the ultraviolet, contiguous conspicuous spectral regions. The anticipated color of the substances involved in specimen effects directly by reflectance or absorbance in the conspicuous range. In certain region of the electromagnetic (EM) spectra, molecules and atoms include in specimen go through electronic transitions [29- 31]. In figure 5 UV-Visible absorption Spectra of Zinc doped Cobalt Ferrite for the variable concentration of Zn^{2+} ions. Fig. 5 shows that the band absorption spectrum of Zinc doped Cobalt Ferrite for multiple concentration values of Zinc (Zn^{2+}) ions as a dopant. The absorbance results of UV Spectra indicate that ($Co_{1-x}Zn_xFe_2O_4$) specimen had symbolic absorbance in the range of 660-900nm wavelength range of the conspicuous region [32, 35]. The absorption of band edge origination for Cobalt Ferrite actually at 1080nm and by doping the specimen using Zinc (Zn^{2+}) ion the value of edge absorption sequentially shifted. The values of absorption region originate for Zinc doped Cobalt Ferrite are 899, 903, 898, 899 and 900 nm for Zn^{2+} concentration ($x=0.1, 0.2, 0.3, 0.4$ and 0.5) correspondingly [36- 38].

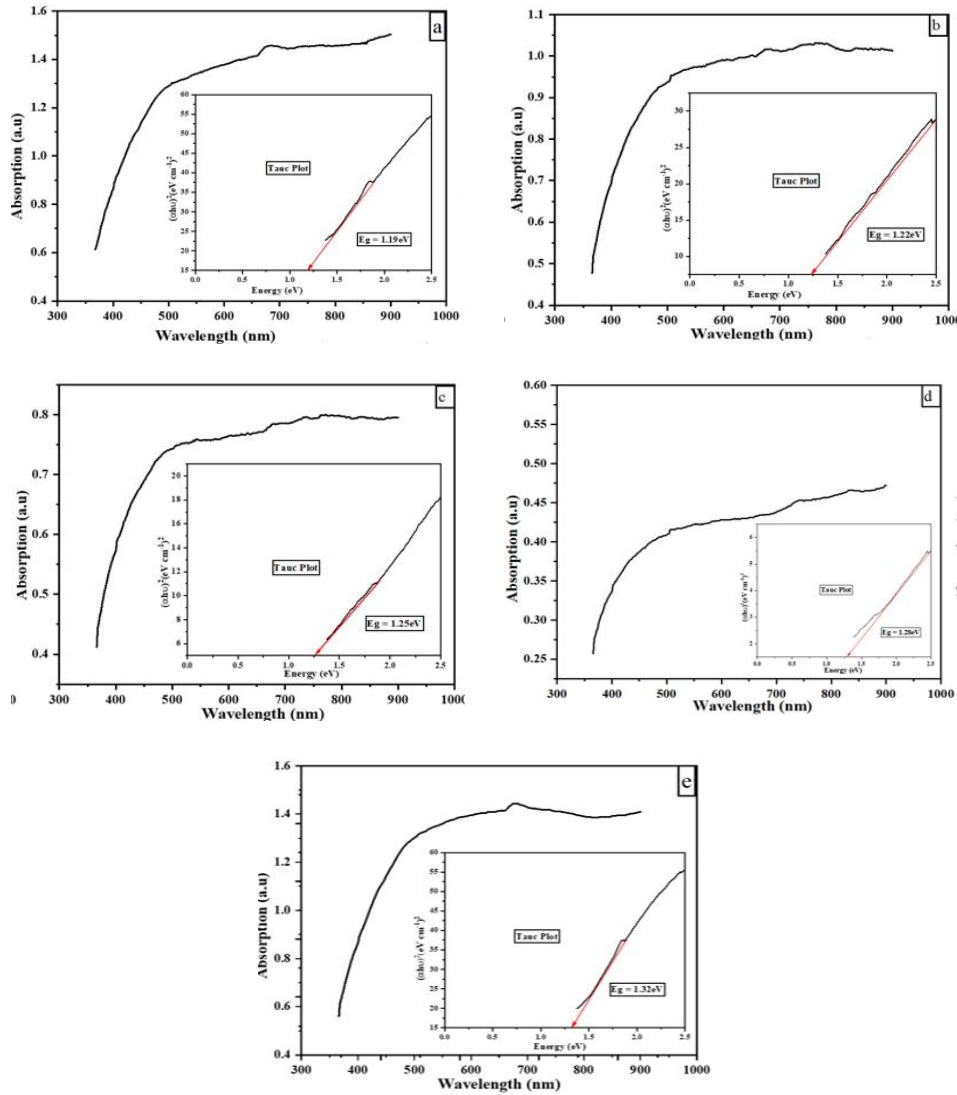


Fig. 4. UV Visible Spectra of absorption for $\text{CoFe}_{2-x}\text{Zn}_x\text{O}_4$ $x=0.1-0.5$.

3.3. Bandgap of Zinc doped Cobalt Ferrite $\text{CoFe}_{2-x}\text{Zn}_x\text{O}_4$

The estimated values of bandgap energy of the specimens of Zinc doped Cobalt Ferrite are extracted from a plot of $(\alpha h\nu)^2$ against energy of photon $(h\nu)$ [39- 42]. The coefficient of optical absorption near the band edge is calculated from Tauc relation using following equation:

$$\alpha h\nu = A(h\nu - E_g)^{1/2} \quad (8)$$

α, h, ν, A, E_g refers to frequency of light, absorption coefficient, Plank's Constant constant of proportionality and energy of bandgap correspondingly. The calculated value of band gap energy contains the estimation of linear portion of the curve attained through plotting $(\alpha h\nu)^2$ against $(h\nu)$ to concentration the energy axis.

Figure 6 approximated the values of bandgap energy 1.19, 1.22, 1.25, 1.27 and 1.32 eV for the concentration of Zinc (Zn^{2+}) ions ($X= 0.1, 0.2, 0.3, 0.4,$ and 0.5) respectively [43]. This phenomenon designated the significant variation in the bandgap energies of samples that occurs because of the effects of doping in the synthesis ($\text{Co}_{1-x}\text{Zn}_x\text{Fe}_2\text{O}_4$) crystal lattices. Increase in band gap energy value through increasing the of Zinc (Zn^{2+}) ions concentration.

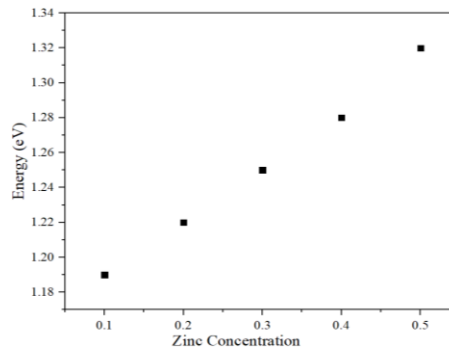


Fig. 5. Linear plot of Zinc concentration against Energy bandgap.

Table 2. Zinc doped-Cobalt Ferrites.

Zinc Concentration	Energy (eV)
0.1	1.19
0.2	1.22
0.3	1.25
0.4	1.27
0.5	1.32

3.4. Morphology Analysis

SEM was used in the micro-structural analysis of the specimens. The specimens were analyzed for grain size and morphology. The SEM micrograph of Zn doped cobalt ferrite is clearly shown in Fig.6. There was a significant change in Zn doped cobalt ferrite morphology by the addition of Zn concentration into the doped cobalt ferrite. The average particle size as measured from SEM images were 42 nm, to 50nm for $\text{CoFe}_{2-x}\text{Zn}_x\text{O}_4$ (Zn doped cobalt ferrites) ($x=0.1-0.5$) respectively at sintered at 500°C for 3h. It is clear from SEM image that particle size of the doped configurations is higher than that of pure cobalt ferrites [44- 48]. The sintering of the cobalt ferrite appears to be significantly different in Zn concentration. When doped in the trivalent Fe^{+3} corner of the zinc doped cobalt ferrite lattice constant generates oxygen vacancies in way to preserve the electrical charge neutrality of the crystal then Zn in a divalent cation (Zn^{+2}) shape. We conclude from SEM image that by increasing the Zn concentration Zn goes into the Fe sites of the cobalt ferrite lattice parameters, more oxygen vacant space are generated. The rate of sintering is improved in presence of oxygen vacancies resulted simplifying grain evolution. (14)

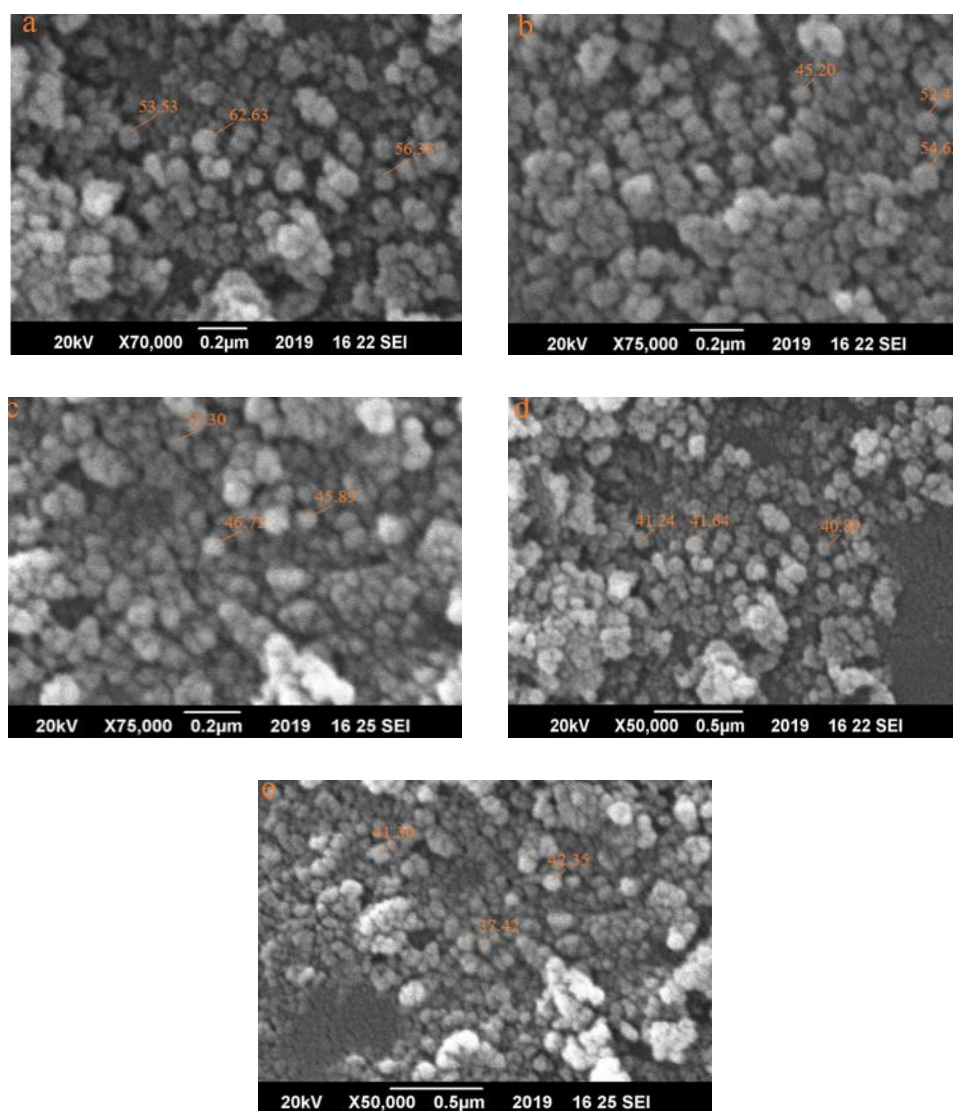


Fig. 6. SEM Morphology of Zinc doped Cobalt Ferrite $\text{CoFe}_{2-x}\text{Zn}_x\text{O}_4$.

4. Conclusions

Cobalt-ferrite (CoFe_2O_4) based nanoparticles are appropriate candidates for electrical, optical and magnetic applications for electrical appliances. In the current study, a co-precipitation technique was used to prepare Zinc doped cobalt ferrites with compositions $\text{CoFe}_{2-x}\text{Zn}_x\text{O}_4$ ($x=0.1-0.5$) at various percentages using Zinc and Co-nitrate as precursors. The analysis of crystal phase structure, hkl planes, average crystalline size, volume and lattice parameters of unit cell of $\text{CoFe}_{2-x}\text{Zn}_x\text{O}_4$ doped (NPs) was carried under X-ray diffraction (XRD). X-ray spectra analysis, FT-IR Spectra, UV Visible Spectra and SEM studies shown that the as synthesized powders were contained of nano-crystallite size (42–53nm) cubic-spinel phase with irregularly-structure.

Calcination at low temperature (80°C) of the precursor followed through sintering (500°C for 3h) consequence in a single phase cubic-spinel shape with average particle size of 42-53nm, as shown by scanning electron micrographs images. Sharp peaks and intense diffraction features in XRD pattern shows that increase in Zn doping concentration in cobalt spinel ferrite increases the crystalline behavior of the cubical spine phase. In cubical structure ferrites crystal lattices the absorption band at low frequency is noticed above 400cm^{-1} but in the range of $300-600\text{cm}^{-1}$ of the

Fourier Transform Infrared bands were attributed to the tremblant of the ions of metal. The absorbance results of UV Spectra indicate that Zinc doped Cobalt Ferrite specimen had symbolic absorbance in the range of 660-900nm wavelength range of the conspicuous region. The Zn-doped cobalt-ferrite have high strain derivative could be a prospective material for electrical devices.

Acknowledgments

This research was funded by the Malaysian Ministry of Higher Education's Fundamental Research Grant [FRGS/1/2019 / STG07 / UTHM/02/5 (FRGS K171)] and University Tun Hussein Onn Malaysia (UTHM), TIER 1 (H218) and GPPS (H423).

References

- [1] T. R. Tatarchuk, M. Bououdina, N. D. Paliychuk, I. P. Yaremiy, V. V Moklyak, J. Alloys Compd. **694**, 777 (2017).
- [2] P. Joy, N. Somaiah, T. V Jayaraman, P. A. Joy, D. Das, Journal of Magnetism and Magnetic Materials Magnetic and magnetoelastic properties of Zn-doped, no. July, 2012.
- [3] H. Anwar, A. Maqsood, I. H. Gul, J. Alloys Compd., 2014.
- [4] M. Arif et al., Test Eng. Manag. **83**(May/June), 22302 (2020).
- [5] M. Q. Hamzah, S. O. Mezan, A. N. Tuama, A. H. Jabbar, M. A. Agam, Int. J. Eng. Technol. **7**, 538 (2018).
- [6] M. Q. Hamzah, A. H. Jabbar, S. O. Mezan, A. N. Tuama, M. A. Agam, AIP Conference Proceedings, 2019.
- [7] S. O. Mezan et al., AIP Conference Proceedings **2151**, 2019.
- [8] A. H. Jabbar, S. O. Mezan, A. N. Tuama, M. Q. Hamzah, A. S. B. Ameruddin, M. A. Agam, AIP Conference Proceedings, 2019.
- [9] R. Kripal, O. Suwalka, N. Lakshmi, K. Venugopalan, Synthesis of chromium substituted nano particles of cobalt zinc ferrites by coprecipitation **59**, 3402 (2005).
- [10] K. M. Batoo et al., Dielectric and low temperature magnetic response of Zn doped cobalt ferrite nanoparticles **055202**(October), 2019.
- [11] T. J. H. Ali, A. A. Jaber, S. Farhan, J. A. Fraih, M. Q. Hamzah, J. Phys. Conf. Ser. **1279**(1), 2019.
- [12] G. M. Mustafa, M. Saleem, S. Atiq, S. Riaz, S. A. Siddiqi, S. Naseem, J. Saudi Chem. Soc. 2018.
- [13] D. R. Mane, D. D. Birajdar, S. Patil, S. E. Shirsath, R. H. Kadam, Redistribution of cations and enhancement in magnetic properties of sol-gel synthesized Cu 0.7 2 **4**, 70 (2011).
- [14] J. J. Vijaya, G. Sekaran, M. Bououdina, Ceram. Int. **41**(1), 15 (2015).
- [15] T. A. Babu, K. V Ramesh, V. R. Reddy, D. L. Sastry, Mater. Sci. Eng. B **228**(November), 175 (2018).
- [16] Y. Yoshida, M. R. Anantharaman, Journal of Magnetism and Magnetic Materials Impact of zinc substitution on the structural and magnetic properties of chemically derived nanosized manganese zinc mixed ferrites **321**, 1092 (2009).
- [17] S. Singh, B. C. Yadav, R. Prakash, B. Bajaj, J. Rock, Appl. Surf. Sci. **257**(24), 10763 (2011).
- [18] M. G. Naseri, E. B. Saion, H. A. Ahangar, A. H. Shaari, M. Hashim, Simple Synthesis and Characterization of Cobalt Ferrite Nanoparticles by a Thermal Treatment Method **2010**.
- [19] Q. Guo et al., Ceram. Int., no. September, 0 (2017).
- [20] T. Dippong, E. Levei, O. Cadar, Journal of Solid State Chemistry **275**(April), 159 (2019).
- [21] N. Sanpo, J. Wang, C. C. Berndt, Effect of Zinc Substitution on Microstructure and Antibacterial Properties of Cobalt Ferrite Nanopowders Synthesized by Sol-gel Methods **537**, 436 (2012).
- [22] A. Manikandan, R. Sridhar, S. A. Antony, S. Ramakrishna, J. Mol. Struct. **1076**, 188 (2014).
- [23] P. Yaseneva, M. Bowker, G. Hutchings, Structural and magnetic properties of Zn-substituted cobalt ferrites prepared by co-precipitation method, 18609 (2011).

- [24] A. Narayanasamy, N. Sivakumar, Influence of mechanical milling and thermal annealing on electrical and magnetic properties of nanostructured Ni – Zn and cobalt ferrites **31**(3), 373 (2008).
- [25] G. Xi, Y. Xi, Effects on magnetic properties of different metal ions substitution cobalt ferrites synthesis by sol – gel auto-combustion route using used batteries **164**, 444 (2016).
- [26] A. Hassadee, T. Jutarosaga, W. Onreabroy, Procedia Engineering Effect of zinc substitution on structural and magnetic properties of cobalt ferrite, 1 (2012).
- [27] S. Sagadevan, J. Podder, I. Das, Synthesis and Characterization of Cobalt Ferrite (CoFe₂O₄) Nanoparticles Prepared by Hydrothermal Method 145–152.
- [28] S. Nasrin, S. M. Hoque, F. Chowdhury, M. M. Hossen, Influence of Zn substitution on the structural and magnetic properties of Co_{1-x}Zn_xFe₂O₄ nano-ferrites, no. September 2016.
- [29] S. Labib, E. Abdeltwab, M. M. El-Okr, Particuology, 1 (2018).
- [30] K. Nadeem, M. Shahid, M. Mumtaz, Prog. Nat. Sci. Mater. Int., 1 (2014).
- [31] A. El Foulani, A. Aamouche, F. Mohseni, J. S. Amaral, D. M. Tobaldi, R. C. Pullar, J. Alloys Compd., 2018.
- [32] I. Ali, Z. Mohamed, M. Alsalheen, Oil Spill Removal from Water by Absorption on Zinc-Doped Cobalt Ferrite Magnetic Nanoparticles **2**(4), 365 (2019).
- [33] M. Sundararajan, L. J. Kennedy, P. Nithya, J. Vijaya, M. Bououdina J. Phys. Chem. Solids, 2017.
- [34] M. A. Agam, M. Q. Hamzah, B. D. Juilis, S. Ashikin, J. A. Yabagi, Int. J. Mech. Prod. Eng. Res. Dev. **10**(3), 213 (2020).
- [35] J. A. Yabagi, M. I. Kimpa, B. L. Muhammad, M. Q. Hamzah, H. K. A. Kadir, M. Arif Agam, Int. J. Nanoelectron. Mater. **13**(2), 263 (2020).
- [36] R. K. Singh et al., Thermal , structural , magnetic and photoluminescence studies on cobalt ferrite nanoparticles obtained by citrate precursor method, 573 (2012).
- [37] P. Khirade, S. D. Birajdar, K. M. Jadhav, Low temperature synthesis of magnesium doped cobalt ferrite nanoparticles and their structural properties, no. March, 2015.
- [38] Z. Karimi, Y. Mohammadifar, H. Shokrollahi, S. Khameneh, G. Youse, L. Karimi, Journal of Magnetism and Magnetic Materials **361**, 150 (2014).
- [39] A. T. Mohd Arif Agam, Nurul Nabilah Awal, Siti Ashikin Hassan, Jibrin Alhaji Yabagi, Maytham Qabel Hamzah, J. Adv. Res. Fluid Mech. Therm. Sci. **66**(2), 125 (2020).
- [40] D. Sharma, N. Khare, Tuning of optical bandgap and magnetization of CoFe₂O₄ thin films Tuning of optical bandgap and magnetization of CoFe₂O₄ thin films **032404**, 1 (2014).
- [41] A. H. Jabbar, H. S. O. Al-janabi, M. Q. Hamzah, S. O. Mezan, A. N. Tumah, A. S. B. Ameruddin, International J. Adv. Sci. Technol. **29**(03), 4913 (2020).
- [42] A. N. Tuama, K. H. Abass, M. Q. Hamzah, S. O. Mezan, M. A. Bin Agam, Test Eng. Manag. **83**(13090), 13090 (2020).
- [43] C. Singh, S. Jauhar, V. Kumar, J. Singh, S. Singhal, Mater. Chem. Phys., 1 (2015).
- [44] N. M. Deraz, A. Alarifi, J. Anal. Appl. Pyrolysis **94**, 41 (2012).
- [45] N. M. Deraz, O. H. Abd-elkader, E. Microscope, E.- Behooth, Structural , Morphological and Magnetic Properties of, **10**, 7138 (2015).
- [46] S. J. Azhagushanmugam, N. Suriyanarayanan, R. Jayaprakash, Mater. Sci. Semicond. Process. **21**, 33 (2014).
- [47] A. N. Tuama, K. H. Abbas, M. Q. Hamzah, S. O. Mezan, A. H. Jabbar, M. A. Agam, J. Adv. Sci. Technol. **29**(03), 5008 (2020).
- [48] S. O. Mezan et al., Int. J. Psychosoc. Rehabil. **4**, 4532 (2020).